OPEN

[18F]PR04.MZ PET/CT Imaging for Evaluation of Nigrostriatal Neuron Integrity in Patients With Parkinson Disease

Carlos Juri, MD, PhD,† Vasko Kramer, PhD,‡§ Patrick J. Riss, PhD,|| Cristian Soza-Ried, PhD,§ Arlette Haeger, MD,§ Rossana Pruzzo, MD,§ Frank Rösch, PhD,¶ Horacio Amaral, MD,‡§ and Pedro Chana-Cuevas, MD**††*

Introduction: Degeneration of dopaminergic, nigrostriatal neurons is the hallmark of Parkinson disease (PD), and PET quantification of dopamine transporters is a widely accepted method for differential diagnosis between idiopathic PD and essential tremor. [18F]PR04.MZ is a new PET tracer with excellent imaging properties allowing for precise quantification of striatal and extrastriatal dopamine transporter. Here we describe our initial experience with [18F]PR04.MZ PET/CT in a larger cohort of healthy controls and PD patients as a proof-of-concept study for this tracer.

Methods: Eighteen healthy subjects, 19 early PD patients (Hoehn-Yahr I–II), and 13 moderate-advanced PD patients (Hoehn-Yahr III–IV) underwent static PET/CT scans 60 to 90 minutes after injection of 5.16 ± 1.03 mCi (191 ± 38 MBq) [18F]PR04.MZ. Specific binding ratios (SBRs) were calculated for caudate nucleus, anterior putamen, posterior putamen, substantia nigra (SNpc), compared between different groups and correlated with clinical ratings.

Results: [18F]PR04.MZ showed very high and specific uptake in the putamen, caudate, and substantia nigra pars compacta and very low nonspecific binding in other brain regions, and SBR values for the control group were 22.3 ± 4.1, 19.1 ± 3.5, and 5.4 ± 1.2, respectively. A reduction of SBR values was observed in all regions and in both initial and moderate PD, ranging from 35% to 89% ($P < 0.001$). The observed pattern of reduction was posterior putamen > anterior putamen > substantia nigra pars compacta > caudate, with contralateral posterior putamen being the most affected region. Rostrocaudal depletion gradient was evident in all PD patients and progression correlated with motor manifestations.

Conclusions: [18F]PR04.MZ PET/CT is a highly sensitive imaging modality for the detection of dopaminergic deficit in nigrostriatal pathways in PD.

Received for publication August 4, 2020; revision accepted October 14, 2020.

From the *Department of Neurology, Facultad de Medicina, Pontificia Universidad Católica de Chile; †Department of Neurology, Hospital Sotero del Río; ‡Nuclear Medicine and PET/CT Center PositronMed; and §Positronpharma SA, Santiago, Chile; ||Department of Chemistry, University of Oslo, Oslo, Norway; ¶Institute of Nuclear Chemistry, Johannes Gutenberg-University, Mainz, Germany; and **Centro de Trastornos del Movimiento; and ††Facultad de Ciencias Médicas, Universidad de Santiago de Chile, Santiago, Chile.

Conflicts of interest and sources of funding: This study was funded by national research grants from CORFO (13PIE-21682) and CONICYT (FONDECYT 11130534). None declared to all authors.

All procedures performed in studies involving human participants were in accordance with the ethical standards of the institutional and national research committee and with the principles of the 1964 Declaration of Helsinki and its later amendments or comparable ethical standards. The study was approved by the regional ethics committee board (CEC SSM Oriente, permit 20140520), and written informed consent has been obtained from all participants.

Correspondence to: Carlos Juri, MD, PhD, Department of Neurology, Facultad de Medicina, Pontificia Universidad Católica de Chile, Diagonal Paraguay 362, Santiago, Chile. E-mail: cajuri@gmail.com.

ISSN: 0363-9762/21/4602–0119
DOI: 10.1097/RLU.0000000000003430

Key Words: [18F]PR04.MZ, dopamine transporter, movement disorders, Parkinson disease, PET imaging

(*Clin Nucl Med* 2021;46: 119–124)

Parkinson disease (PD) is characterized by the pathologic deposition of α-synuclein aggregates and the subsequent degeneration of dopaminergic neurons.[1] The availability of reliable biomarkers for PD is critical to establish early or even presymptomatic diagnosis, to track dopaminergic depletion, and to evaluate disease-modifying therapies, aimed to alter the course of progression.[2–4] Molecular imaging techniques such as PET and SPECT are used worldwide to evaluate movement disorder patients for this purpose.[5] In order to evaluate new biomarkers for PET, it is important to determine their ability to reliably detect dopaminergic deficits, as well as to describe the pattern of neuronal loss and its progression over time.[5–8]

Although numerous neurotransmitter systems are affected in PD, studies have shown a direct relationship between dopaminergic nigrostriatal depletion and the onset and progression of motor manifestations, in particular rigidity and bradykinesia.[9,10] While most studies focused on striatal dopaminergic depletion, recent data suggest that dopaminergic activity in the substantia nigra pars compacta (SNpc) shows better correlations with motor manifestations and dopaminergic cell counts, especially in more advanced disease.[11,12] The researchers further showed that this applies in particular for binding potentials in SNpc for both presynaptic dopamine transporters (DATs) and vesicular monoamine transporters, measured with [11C]CFT and [11C]DTBZ, respectively. Consequently, PET imaging of the SNpc may provide additional value for the evaluation of PD patients.

The DAT is an established target for diagnostic imaging in movement disorders, and the only approved radiopharmaceutical to date is the SPECT tracer Datscan (also known as [123I]Ioflupan or [123I]FP-CIT).[13] Its clinical application is indicated to assist in the evaluation of adult patients with suspected parkinsonian syndromes (PSs) and may be used to differentiate essential tremor from tremor due to PS (idiopathic PD, multiple system atrophy, and progressive supranuclear palsy).[13–15] While DAT SPECT imaging is well established in clinical practice and provides good diagnostic accuracy, highly selective PET tracers may offer significant advantages, such as improved sensitivity, specificity, image quality and more convenient imaging protocols.[16–18] These improvements may be of particular relevance for reliable evaluation of the midbrain region, where DAT availability is lower.[19,20] Several promising 18F-labeled PET imaging compounds, such as [18F]FP-CIT, [18F]FE-PE2I, and [18F]LBT-999, have been developed but are still in early clinical development.[17,21–23]

Recently, [18F]PR04.MZ has been described as a new PET imaging agent with an improved affinity (half maximal inhibitory concentration (IC_{50}) = 3.3 nM) and selectivity profile (74-fold over serotonin transporter (SERT), 10-fold over norepinephrine transporter (NET)) for DAT.[24,25] The clinical potential of this new tracer was highlighted by the excellent imaging properties in a case study of

Holmes tremor[26] and the clinical application for detection of nigrostriatal degeneration in patients under evaluation for movement disorders.[27] The pharmacokinetic evaluation of [^{18}F]PR04.MZ showed very high specific uptake in striatal and midbrain regions, excellent imaging contrast, and stable, reliable quantification outcomes within a reasonable time frame.[16]

Therefore, in the present study, we aimed to evaluate the diagnostic accuracy of [^{18}F]PR04.MZ PET/CT in a larger cohort of healthy controls (HCs) and PD patients as a proof-of-concept study for the clinical utility of this new tracer.

METHODS

Study Population

The prospective study was approved by the regional ethics committee board (CEC-SSM-Oriente, permit 20140520), and written informed consent has been obtained from all participants.

Eighteen HCs (aged 56.6 ± 8.2 years; range, 41–74 years; 9 male and 9 female patients) were included in the study. Inclusion criteria were the age of 40 to 80 years and showing no signs of neurological or psychiatric disorders as confirmed by standard neurological examination. Exclusion criteria were smoking and the use of psychoactive substances. Subjects fasted for at least 12 hours before tracer injection, including caffeine restriction.

A total of 32 PD patients (aged 55.2 ± 13.7 years; range, 26–73 years) were recruited, diagnosed according to London Brain Bank criteria, and classified as mild (n = 19, 5 female and 14 male patients) or moderate (n = 13, 6 female and 7 male patients) according to Hoehn-Yahr (HY) OFF stage (mild: HY I–II and moderate: HY III–IV). Exclusion criteria were atypical parkinsonism, cognitive decline, depression, and use of antidepressants in the past 2 months or dopamine blockers in the last 6 months. For detailed subject demographics, see Table 1.

PET Acquisition

[^{18}F]PR04.MZ was produced under GMP-compliant conditions as previously described.[16] The mean ± SD of the administered activity was 5.16 ± 1.03 mCi (191 ± 38 MBq; range, 88.8–322 MBq). There were no adverse or clinically detectable pharmacologic effects in any of the 50 subjects, and no significant changes in vital signs were observed. All images were acquired on a state-of-the-art whole body PET/CT scanner (Biograph mCT20 or mCT Flow; Siemens Healthineers, Erlangen Germany), and head movement was minimized using a head immobilization system. For HCs, a low-dose CT scan was performed for attenuation correction followed by a dynamic PET scan acquired in LIST mode for 90 minutes, started simultaneously with tracer injection. For PD patients, studies were conducted in OFF condition, 18 h after the last dose of levodopa, if applicable. Patients were injected with [^{18}F]PR04.MZ and allowed to rest for 55 minutes before being placed head-first supine the PET/CT scanner. A low-dose CT for attenuation correction was performed before a static PET acquisition acquired in LIST mode for 30 minutes from 60 to 90 minutes postinjection (p.i.).

TABLE 1. Demographics and Clinical Ratings of Participants

	HC	Mild PD (HY I–II)	Moderate PD (HY III–IV)	*P*
Age, y	56.6 ± 8.2	53.8 ± 14.6	57.1 ± 12.5	NS
Male/female, n	9/9	14/5	7/6	NS
Disease duration, y	NA	3.16 ± 2.20	7.7 ± 4.3	<0.01
L-DOPA equivalents, mg	NA	142.73 ± 204.8	729.7 ± 467.4	<0.001
UPDRS III	NA	12.53 ± 6.58	24.0 ± 8.50	<0.001
Akinesia	NA	5.95 ± 3.85	11.31 ± 4.00	<0.001
Rigidity	NA	2.60 ± 2.70	6.70 ± 1.75	<0.001
Tremor	NA	2.32 ± 2.03	1.15 ± 1.41	NS
Mod. HY stage	NA	1.39 ± 0.49	3.15 ± 0.69	<0.001

All data are expressed as mean ± SD values.

NA, not applicable; NS, not statistically significant.

Image Postprocessing and Analysis

PET images were corrected (TrueX software) for random, scatter, attenuation, and time-of-flight and reconstructed by an ordered subset expectation maximization algorithm (2 iterations and 21 subsets) followed by postreconstruction smoothing (Gaussian, 4 mm full-width half-maximum). Images consisted of 110 planes of 256 × 256 voxels of 1.59 × 1.59 × 1.5 mm^3. The 90-minute dynamic PET scans, acquired for HCs, were reframed into 38 static frames (6 × 10, 6 × 20, 7 × 60, 5 × 120, 14 × 300 seconds), whereas PET scans acquired for PD patients were reframed into 6 static frames of 300 seconds each. All further analyses were performed using the Pmod quantification software (PMOD v3.4, Pmod Technologies LLC, Zurich, Switzerland). PET images were reviewed, corrected for motion, and averaged for the period of 60 to 90 minutes p.i. Images were coregistered to CT scans and normalized to Montreal Neurological Institute space using an in-house CT template. Volumes of interest (VOIs) were outlined from an in-house VOI template for relevant brain VOIs (anterior, posterior, and total putamen; caudate nucleus; SNpc; and cerebellum—all divided into left, right, and total). SUVs were obtained by normalizing radioactive concentrations in VOIs to the injected dose per body weight. Specific binding ratios (SBRs) were calculated from SUVs as follows:

$$\mathrm{SBR} = (\mathrm{SUV}_{\mathrm{mean}}\ \mathrm{region} - \mathrm{SUV}_{\mathrm{mean}}\ \mathrm{cerebellum})/\mathrm{SUV}_{\mathrm{mean}}\ \mathrm{cerebellum}.$$

To compare differences between both hemispheres, asymmetry indices (AI) were calculated for all regions from SBRs as follows:

$$\mathrm{AI} = \mathrm{I}\left(\mathrm{SBR}_{\mathrm{left}} - \mathrm{SBR}_{\mathrm{right}}\right)/\left(\mathrm{SBR}_{\mathrm{left}} + \mathrm{SBR}_{\mathrm{right}}\right)\mathrm{I} \times 200.$$

Finally, ratios between anterior and posterior putamen were calculated as a measure of a rostrocaudal gradient (RCG), often found in PD patients, as follows:

$$\mathrm{RCG} = \mathrm{SBR}_{\mathrm{anterior\ putamen}}/\mathrm{SBR}_{\mathrm{posterior\ putamen}}$$

Statistical Analysis

The differences in [^{18}F]PR04.MZ-SBR were obtained from the analysis of VOIs in control and PD groups, using a one-way analysis of variance with motor status as a within-subject factor.

Differences in striatal regions among PD patients were assessed using post hoc analysis on another one-way analysis of variance with motor status as within-subject factor, using the Bonferroni correction for multiple comparisons and the Kruskal-Wallis and the Dunn multiple comparison as a post hoc nonparametric test. To compare between mild and moderate PD, we used 2-tailed unpaired Student *t* test and Wilcoxon test as a nonparametric test. To assess the equality of variances between groups, the Levene test was used. Shapiro-Wilk test and Q-Q plots were used to test for normal distribution of the data. All statistics were performed with SPSS software version 16.0 software for Windows (SPSS Inc, Chicago, Ill). Two-sided *P* values of less than 0.05 and 0.01 were considered significant.

RESULTS

In the age-matched HC group, [^{18}F]PR04.MZ showed very high uptake, low off-target binding, and excellent visual contrast

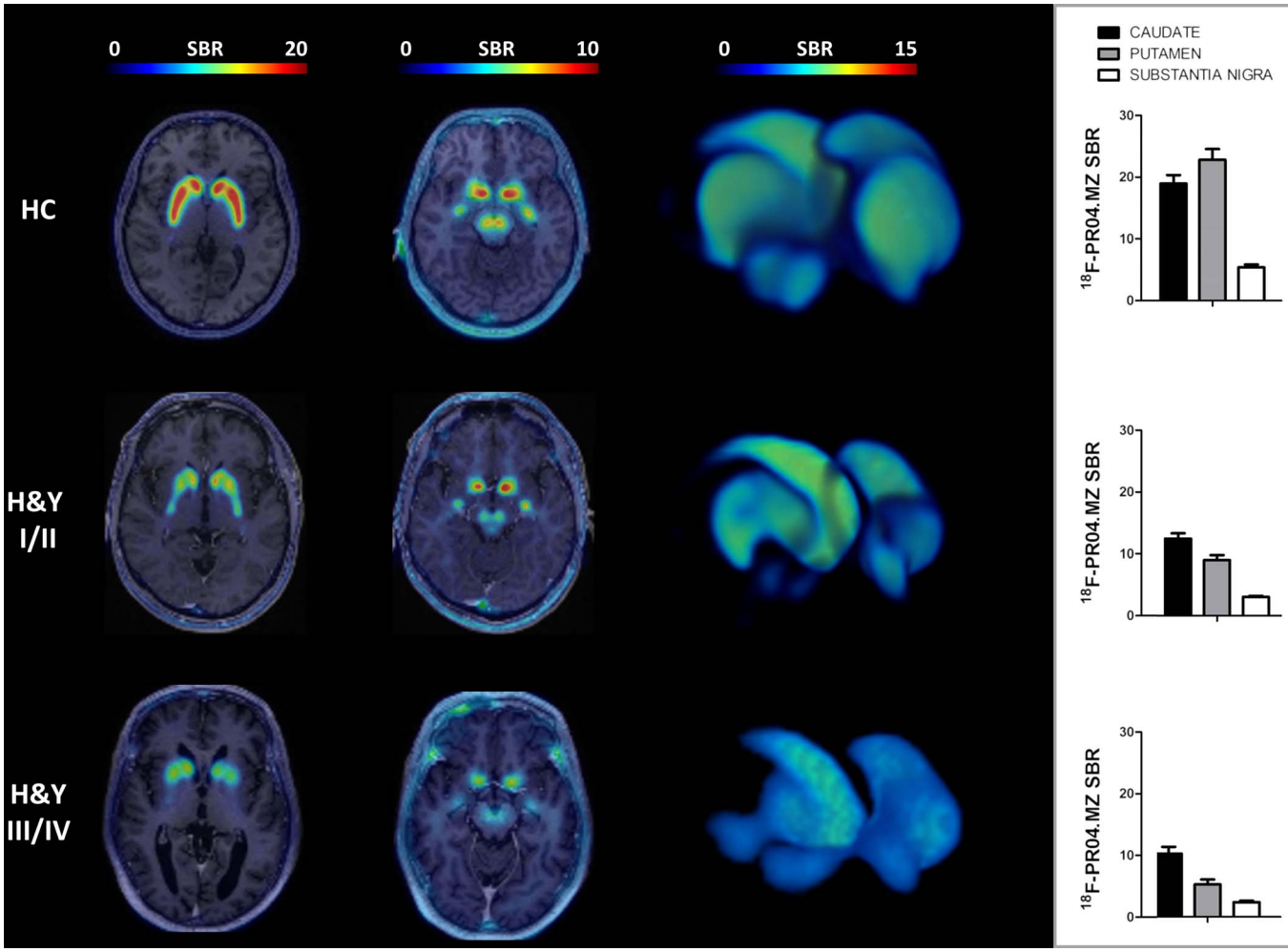

FIGURE 1. Transversal view of PET images coregistered to corresponding T1-weighted MRIs in striatal region (first column) and midbrain region (second column) for HCs (above), mild PD (middle), and moderate PD (below). Three-dimensional rendered images of [18F]PR04.MZ uptake (third column; cutoff for render: SBR 2–15) and mean regional SBR values (fourth column) of HC and PD patients.

in striatal and midbrain regions and in all subjects (Fig. 1). Highest uptake was observed in anterior putamen (SBR = 22.7 ± 4.1; range, 14.6–32.5) followed by posterior putamen (SBR = 21.9 ± 4.2; range, 14.7–31.7) and caudate nucleus (SBR = 19.1 ± 3.5; range, 13.7–26.6). In the midbrain region, SNpc was separated clearly by visual assessment from surrounding tissues, and specific uptake was about 5-fold higher than in cerebellum (SBR = 5.39 ± 1.23; range, 2.48–7.06). There was no relevant asymmetry in uptake (AI = 4.4 ± 3.4, 3.2 ± 2.0, 5.1 ± 4.2, and 4.1 ± 3.1) in caudate, anterior putamen, posterior putamen, or SNpc, respectively, and no rostrocaudal gradient was observed in HCs (RCG = 1.04 ± 0.08; range, 0.93–1.18) (Table 2).

As expected, uptake of [18F]PR04.MZ was decreased in all striatal regions and midbrain in all PD patients compared with HCs ($P < 0.001$). The most affected side was the posterior putamen, contralateral to the primarily affected side of the body, with a decrease of 80% for patients with mild and 89% in moderate PD. Specific binding ratios were lower for all other regions with a reduction of 50%, 37%, and 44% in mild PD patients and 68%, 46%, and 56% in moderate PD patients in anterior putamen, caudate nucleus, and SNpc, respectively ($P < 0.001$). Specific binding ratio values for SNpc in mild (SBR = 3.03 ± 0.83; range, 1.61–4.64) and moderate (SBR = 2.36 ± 0.71; range, 1.09–3.38) PD patients were decreased, as compared with HC ($P < 0.001$). Among both PD groups, SBR values of anterior putamen were lower in moderate PD ($P < 0.05$) (Table 2). Asymmetrical uptake of [18F]PR04.MZ was evident in all regions and most severe in posterior putamen with AI values of 47.5 ± 27.5 and 43.1 ± 30.1 in mild and moderate PD, respectively. Further, a rostrocaudal gradient was observed for [18F]PR04.MZ uptake in patients with mild and moderate PD, which was most severe for the contralateral putamen with RCG values of 2.43 ± 0.56 and 2.76 ± 0.77, respectively, and which was not evident in HCs ($P < 0.001$).

The Unified Parkinson's Disease Rating Scale III (UPDRS III) score and rigidity and akinesia subscores showed a negative correlation for SBR in caudate, putamen, and SNpc. Unexpectedly, a positive correlation was found between tremor and SBR in the 3 regions (Fig. 2).

DISCUSSION

Diagnostic, molecular imaging is a valuable tool to evaluate movement disorder patients, and in addition to [123I]FP-CIT, new, specific PET tracers have emerged in recent years.[21–23] Related to the advantages mentioned previously of PET over SPECT,[18] those might improve diagnostic accuracy or even serve as predictive

TABLE 2. SBR Values for Different Brain Regions and %-Decline for Mild and Moderate PD Patients

	HC	Mild PD (HY I–II)			Moderate PD (HY III–IV)			
	SBR	SBR	Decline	*P*	SBR	Decline	*P*	*P* (Mild vs Moderate)
Caudate	19.14 ± 3.51	12.08 ± 3.61	37%	<0.001	10.31 ± 3.48	46%	<0.001	NS
C. contralateral	NA	11.69 ± 3.40	39%	<0.001	9.84 ± 3.12	49%	<0.001	NS
C. ipsilateral	NA	12.52 ± 3.80	35%	<0.01	10.78 ± 4.02	44%	<0.001	NS
Putamen anterior	22.68 ± 4.10	11.43 ± 4.16	50%	<0.001	7.24 ± 3.54	68%	<0.001	<0.05
P. anterior contralateral	NA	10.34 ± 4.02	54%	<0.001	6.29 ± 2.72	72%	<0.001	<0.05
P. anterior ipsilateral	NA	12.51 ± 4.54	45%	<0.001	8.18 ± 4.45	64%	<0.001	<0.05
Putamen posterior	21.87 ± 4.21	5.58 ± 2.29	74%	<0.001	3.10 ± 1.64	86%	<0.001	NS
P. posterior contralateral	NA	4.36 ± 1.88	80%	<0.001	2.36 ± 0.91	89%	<0.001	NS
P. posterior ipsilateral	NA	6.80 ± 3.11	69%	<0.001	3.83 ± 2.51	82%	<0.001	NS
Substantia nigra	5.39 ± 1.23	3.03 ± 0.83	44%	<0.001	2.36 ± 0.71	56%	<0.001	NS
SN contralateral	NA	2.86 ± 0.75	47%	<0.001	2.27 ± 0.61	58%	<0.001	NS
SN ipsilateral	NA	3.21 ± 0.92	40%	<0.001	2.43 ± 0.83	55%	<0.001	NS
Asymmetry	**AI**	**AI**		***P***	**AI**		***P***	***P* (Mild vs Moderate)**
Caudate	4.41 ± 3.41	7.20 ± 5.44		NS	19.95 ± 8.42		<0.001	<0.001
Putamen anterior	3.17 ± 1.96	22.51 ± 15.87		<0.001	32.21 ± 17.12		<0.001	NS
Putamen posterior	5.12 ± 4.24	47.47 ± 27.45		<0.001	43.12 ± 30.05		<0.001	NS
Substantia nigra	4.13 ± 3.09	11.27 ± 6.72		<0.01	12.38 ± 9.88		<0.01	NS
Rostrocaudal Gradient	**Anterior/Posterior**	**Anterior/Posterior**		***P***	**Anterior/Posterior**		***P***	***P* (Mild vs Moderate)**
Putamen	1.04 ± 0.08	2.12 ± 0.51		<0.001	2.46 ± 0.53		<0.001	NS
P. contralateral	NA	2.43 ± 0.56		<0.001	2.76 ± 0.77		<0.001	NS
P. ipsilateral	NA	1.98 ± 0.61		<0.001	2.35 ± 0.72		<0.001	NS

AI and RCG values for HCs and patients. All data are expressed as mean ± SD values.

NA, not applicable; NS, not statistically significant.

markers. This was exemplified in a recent study demonstrating that anterior-to-posterior gradient and right-to-left asymmetry of striatal DAT availability, measured by [^{18}F]FP-CIT-PET, predicted the development of levodopa-induced dyskinesia.[28] Such regional uptake patterns might be difficult to derive from SPECT images because of the lower spatial resolution. Here we found similar patterns (RCG and AI) in our patient population, but if this correlates with the onset of levodopa-induced dyskinesia in later stages remains to be seen after clinical follow-up.

In this prospective study, we aimed to evaluate the diagnostic accuracy of PET imaging with [^{18}F]PR04.MZ in a larger cohort of HCs and PD patients. Previous contributions from our group evaluated the pharmacokinetic profile of [^{18}F]PR04.MZ and validated the reliability of the static imaging protocol applied here to evaluate larger patient groups. Thereby SBR values from 60 to 90 minutes p.i. were found to provide reliable quantitative estimates, with errors of less than 5% of peak SBRs reached during the study and for both striatal and nigral regions.[16]

Patients with PD with essential clinical features already show a loss of 70% to 80% of striatal nerve terminals and 50% to 60% of SNpc neurons.[29–31] In contrast, patients in prodromal stages and without motor symptoms may show less severe degeneration of nigrostriatal neurons, emphasizing that high sensitivity is particularly relevant in this population. Our study shows that PET/CT with [^{18}F]PR04.MZ was able to detect a loss of DAT availability in early PD stages, and SBR values were negatively correlated with UPDRS III score, rigidity, and akinesia subscores.

Precise quantification of DAT is particularly challenging in the midbrain region, where other monoamine transporters such as SERT and NET are also expressed in relevant concentrations. A recent study investigated the DAT density in striatum versus midbrain region in patients with PS using [^{123}I]FP-CIT SPECT imaging, concluding that midbrain uptake did not correlate with motor symptoms.[32] In contrast, our data show that [^{18}F]PR04.MZ is able to detect loss of dopaminergic activity in the SNpc, differentiating patients from HCs, and that this loss correlates with disease severity and motor symptoms. These results demonstrate the limitations of radiotracers with a considerable affinity toward off-targets such as SERT and NET, contributing to nonspecific uptake and confounding quantitative results, especially in SNpc. A significant advantage of [^{18}F]PR04.MZ is the high in vitro selectivity for DAT over SERT (74-fold) and NET (10-fold), and we can therefore assume that the signal measured by PET/CT in SNpc is specific for DAT. FP-CIT, in comparison, measured in the same assay, revealed a significant affinity toward SERT (IC_{50} = 110 ± 64 nM) and only 4-fold selectivity for DAT over SERT.[33]

Evidence suggests that dopaminergic activity measured in the SNpc correlates better than striatal activity with the degree of neuronal cell loss[5] and is probably a better biomarker for evaluating progression in more advanced PD.[11] Moreover, several efforts have been made in recent years to develop PET tracers to detect α-synuclein aggregates in the early stages of PD.[34–36] PET imaging of the pathological buildup of Lewy bodies, cell death of dopaminergic neurons in SNpc, and their correlation may be imperative for our understanding of the disease.

The intermediate results in the present study indicate that SBR values in SNpc may serve as a useful biomarker at mild to moderate stages of the disease. [^{18}F]PR04.MZ-PET provided good

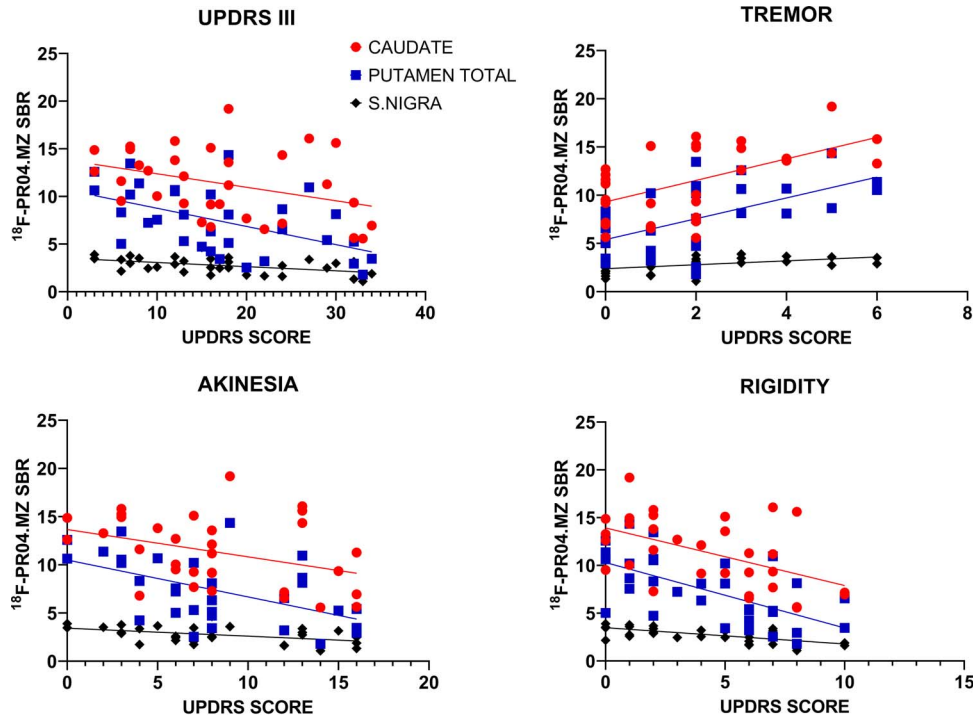

FIGURE 2. [18F]PR04MZ SBRs, UPDRS III, and UPDRS motor subscores in PD patients. The scatterplots and fitted curves are shown for UPDRS III (total motor score) and also for tremor, rigidity, and akinesia subscores of UPDRS III. All curves with $P < 0.05$.

visualization and estimates for DAT in SNpc. There was an inverse relationship between reduced SBR, bradykinesia, and rigidity in the contralateral side. These findings were evident in the putamen, mostly in the posterior putamen, caudate, and SNpc. An unexpected finding was the positive correlation of tremor score with dopaminergic activity (Fig. 2). There is a large body of evidence on both studies with dopaminergic radioligands and neuropathological studies, showing a lack of relationship between tremor and dopaminergic loss.[37–39] Probably studies in larger PD populations, including more patients with tremor, would be needed to confirm this finding.

Similar to other presynaptic dopaminergic radioligands, uptake of [18F]PR04.MZ in PD patients exhibited a rostrocaudal gradient, with a clear asymmetry between both hemispheres and higher contralateral depletion relative to the primarily affected hemibody.[40,41] Further, the exceptionally high target-to-background ratio and uptake in striatal regions may open the door for adapted imaging protocols with significantly reduced doses while maintaining the same image quality.

Despite the excellent initial results with [18F]PR04.MZ PET/CT in the current study, there were some minor limitations such as the relatively small number of participants and the absence of late-stage PD patients and patients with essential tremor. Also, long-term clinical follow-up was not yet available to estimate sensitivity and specificity as endpoint. In prospective longitudinal studies, we aim to increase our study population and evaluate the use of [18F]PR04.MZ as a progression marker further and to establish the role of nigral DAT availability in PD progression.

CONCLUSIONS

PET/CT imaging with [18F]PR04.MZ provides reliable quantification of DAT, and SBRs reveal a good correlation with the clinical severity of PD. Thus, imaging with [18F]PR04.MZ provides the clinical potential to assist in the evaluation of patients with suspicion of PD and other movement disorders.

ACKNOWLEDGMENTS

The authors thank Jonathan Flores and Alejandra Fabre for their assistance with PET imaging and Carlos Elgueta and Jessica Ribbeck for radiopharmaceutical production.

REFERENCES

1. Dickson DW, Braak H, Duda JE, et al. Neuropathological assessment of Parkinson's disease: refining the diagnostic criteria. *Lancet Neurol*. 2009; 8:1150–1157.
2. Booij J, Knol RJ. SPECT imaging of the dopaminergic system in (premotor) Parkinson's disease. *Parkinsonism Relat Disord*. 2007;13(suppl 3):S425–S428.
3. Antonini A, Biundo R. Parkinson disease: can dopamine transporter imaging define early PD? *Nat Rev Neurol*. 2014;10:432–433.
4. Weingarten CP, Sundman MH, Hickey P, et al. Neuroimaging of Parkinson's disease: expanding views. *Neurosci Biobehav Rev*. 2015;59:16–52.
5. Strafella AP, Bohnen NI, Perlmutter JS, et al. Molecular imaging to track Parkinson's disease and atypical parkinsonisms: new imaging frontiers. *Mov Disord*. 2017;32:181–192.
6. Algarni MA, Stoessl AJ. The role of biomarkers and imaging in Parkinson's disease. *Expert Rev Neurother*. 2016;16:187–203.
7. Brooks DJ, Frey KA, Marek KL, et al. Assessment of neuroimaging techniques as biomarkers of the progression of Parkinson's disease. *Exp Neurol*. 2003;184(suppl 1):68–79.
8. Loane C, Politis M. Positron emission tomography neuroimaging in Parkinson's disease. *Am J Transl Res*. 2011;3:323–341.
9. Blesa J, Juri C, Collantes M, et al. Progression of dopaminergic depletion in a model of MPTP-induced parkinsonism in non-human primates. An (18)F-DOPA and (11)C-DTBZ PET study. *Neurobiol Dis*. 2010;38:456–463.
10. Kish SJ, Shannak K, Hornykiewicz O. Uneven pattern of dopamine loss in the striatum of patients with idiopathic Parkinson's disease. Pathophysiologic and clinical implications. *N Engl J Med*. 1988;318:876–880.
11. Karimi M, Tian L, Brown CA, et al. Validation of nigrostriatal positron emission tomography measures: critical limits. *Ann Neurol*. 2013;73:390–396.

12. Brown CA, Karimi MK, Tian L, et al. Validation of midbrain positron emission tomography measures for nigrostriatal neurons in macaques. *Ann Neurol*. 2013; 74:602–610.
13. Isaacson SH, Fisher S, Gupta F, et al. Clinical utility of DaTscan™ imaging in the evaluation of patients with parkinsonism: a US perspective. *Expert Rev Neurother*. 2017;17:219–225.
14. Catafau AM, Tolosa E, DaTscan Clinically Uncertain Parkinsonian Syndromes Study Group. Impact of dopamine transporter SPECT using ^{123}I-ioflupane on diagnosis and management of patients with clinically uncertain parkinsonian syndromes. *Mov Disord*. 2004;19:1175–1182.
15. O'Brien JT, Oertel WH, McKeith IG, et al. Is ioflupane I123 injection diagnostically effective in patients with movement disorders and dementia? Pooled analysis of four clinical trials. *BMJ Open*. 2014;4:e005122.
16. Kramer V, Juri C, Riss PJ, et al. Pharmacokinetic evaluation of [(18)F]PR04. MZ for PET/CT imaging and quantification of dopamine transporters in the human brain. *Eur J Nucl Med Mol Imaging*. 2020;47:1927–1937.
17. Jakobson Mo S, Axelsson J, Jonasson L, et al. Dopamine transporter imaging with [(18)F]FE-PE2I PET and [(123)I]FP-CIT SPECT—a clinical comparison. *EJNMMI Res*. 2018;8:100.
18. Bateman TM. Advantages and disadvantages of PET and SPECT in a busy clinical practice. *J Nucl Cardiol*. 2012;19(suppl 1):3–11.
19. Shumay E, Fowler JS, Volkow ND. Genomic features of the human dopamine transporter gene and its potential epigenetic states: implications for phenotypic diversity. *PLoS One*. 2010;5:e11067.
20. Block ER, Nuttle J, Balcita-Pedicino JJ, et al. Brain region-specific trafficking of the dopamine transporter. *J Neurosci*. 2015;35:12845–12858.
21. Yaqub M, Boellaard R, van Berckel BN, et al. Quantification of dopamine transporter binding using [^{18}F]FP-beta-CIT and positron emission tomography. *J Cereb Blood Flow Metab*. 2007;27:1397–1406.
22. Sasaki T, Ito H, Kimura Y, et al. Quantification of dopamine transporter in human brain using PET with ^{18}F-FE-PE2I. *J Nucl Med*. 2012;53:1065–1073.
23. Chalon S, Vercouillie J, Payoux P, et al. The story of the dopamine transporter PET tracer LBT-999: from conception to clinical use. *Front Med (Lausanne)*. 2019;6:90.
24. Riss PJ, Debus F, Hummerich R, et al. Ex vivo and in vivo evaluation of [^{18}F] PR04.MZ in rodents: a selective dopamine transporter imaging agent. *ChemMedChem*. 2009;4:1480–1487.
25. Riss PJ, Hooker JM, Shea C, et al. Characterisation of [^{11}C]PR04.MZ in Papio anubis baboon: a selective high-affinity radioligand for quantitative imaging of the dopamine transporter. *Bioorg Med Chem Lett*. 2012; 22:679–682.
26. Juri C, Chana P, Kramer V, et al. Imaging nigrostriatal dopaminergic deficit in Holmes tremor with ^{18}F-PR04.MZ-PET/CT. *Clin Nucl Med*. 2015;40:740–741.
27. Chana P, Juri C, Kramer V, et al. Quantification of striatal dopamine transporters with [^{18}F]PR04.MZ in patients with progressive supranuclear palsy and Parkinson's disease. *Mov Disord*. 2016;31.
28. Chung SJ, Yoo HS, Lee HS, et al. The pattern of striatal dopamine depletion as a prognostic marker in de novo Parkinson disease. *Clin Nucl Med*. 2018; 43:787–792.
29. Bernheimer H, Birkmayer W, Hornykiewicz O, et al. Brain dopamine and the syndromes of Parkinson and Huntington clinical, morphological and neurochemical correlations. *J Neurol Sci*. 1973;20:415–455.
30. Fearnley JM, Lees AJ. Striatonigral degeneration. A clinicopathological study. *Brain*. 1990;113(Pt 6):1823–1842.
31. Fearnley JM, Lees AJ. Ageing and Parkinson's disease: substantia nigra regional selectivity. *Brain*. 1991;114:2283–2301.
32. Matesan MC, Cross DJ, Lewis DH, et al. Differential alterations of dopamine transporter in the striatum and midbrain in patients with parkinsonian syndrome. *Clin Nucl Med*. 2015;40:191–194.
33. Riss PJ, Hummerich R, Schloss P. Synthesis and monoamine uptake inhibition of conformationally constrained 2beta-carbomethoxy-3beta-phenyl tropanes. *Org Biomol Chem*. 2009;7:2688–2698.
34. Bagchi DP, Yu L, Perlmutter JS, et al. Binding of the radioligand SIL23 to α-synuclein fibrils in Parkinson disease brain tissue establishes feasibility and screening approaches for developing a Parkinson disease imaging agent. *PLoS One*. 2013;8:e55031.
35. Fodero-Tavoletti MT, Mulligan RS, Okamura N, et al. In vitro characterisation of BF227 binding to alpha-synuclein/Lewy bodies. *Eur J Pharmacol*. 2009;617:54–58.
36. Chu W, Zhou D, Gaba V, et al. Design, synthesis, and characterization of 3-(benzylidene)indolin-2-one derivatives as ligands for α-synuclein fibrils. *J Med Chem*. 2015;58:6002–6017.
37. Kraemmer J, Kovacs GG, Perju-Dumbrava L, et al. Correlation of striatal dopamine transporter imaging with post mortem substantia nigra cell counts. *Mov Disord*. 2014;29:1767–1773.
38. Dirkx MF, den Ouden HE, Aarts E, et al. Dopamine controls Parkinson's tremor by inhibiting the cerebellar thalamus. *Brain*. 2017;140:721–734.
39. Pirker W. Correlation of dopamine transporter imaging with parkinsonian motor handicap: how close is it? *Mov Disord*. 2003;18(suppl 7):S43–S51.
40. Nandhagopal R, Kuramoto L, Schulzer M, et al. Longitudinal progression of sporadic Parkinson's disease: a multi-tracer positron emission tomography study. *Brain*. 2009;132:2970–2979.
41. Moore RY, Whone AL, McGowan S, et al. Monoamine neuron innervation of the normal human brain: an ^{18}F-DOPA PET study. *Brain Res*. 2003; 982:137–145.